

# Sustained-Release Esketamine Based Nanoparticle-Hydrogel Delivery System for Neuropathic Pain Management

Hao Zhang<sup>1,\*</sup>, Ping Zhou<sup>1,\*</sup>, Yi Jiang<sup>1</sup>, Liu Li<sup>1</sup>, Fei Ju<sup>2</sup>, Quan Cheng<sup>1</sup>, You Lang Zhou<sup>2</sup>, Yuan Zhou<sup>1</sup>

<sup>1</sup>Department of Pain, Affiliated Hospital of Nantong University, Medical School of Nantong University, Nantong, People's Republic of China; <sup>2</sup>Research Center of Clinical Medicine, Affiliated Hospital of Nantong University, Nantong, People's Republic of China

\*These authors contributed equally to this work

Correspondence: Yuan Zhou; You Lang Zhou, Tel +86 0513 85052222; +86 0513 85052488, Email nina\_shine@126.com; zhouyoulang@ntu.edu.cn

**Introduction:** Esketamine, one of the few non-opioid potent analgesics, has demonstrated efficacy in the treatment of various chronic pain, particularly neuropathic pain. However, its potential clinical applications are confined due to its short half-life and severe side effects including delirium, hallucinations, and other psychiatric symptoms. Here, we reported a nanosized drug delivery system for sustained-release esketamine based on polylactic-co-glycolic acid (PLGA) nanoparticles and hyaluronic acid (HA) hydrogel.

**Results:** In this study, esketamine in the delivery system was continuously released in vitro for at least 21 days, and spinal nerve root administration of the delivery system successfully attenuated (spinal nerve ligation) SNL-induced pain hypersensitivity for at least 14 days. Notably, the excitability of neurons in murine dorsal root ganglion (DRG) was inhibited and the activation of astrocytes in the spinal cord was additionally reduced after administration. Finally, there was no obvious pathophysiological change in the nerves at the administration site after treatment at 14 days.

**Conclusion:** These results indicate that the sustained-release esketamine based on the nanoparticle-hydrogel delivery system can safely produce a lasting analgesic effect on SNL mice, and its mechanism might be related to modulating the activation of astrocytes in the spinal cord and inhibiting the excitability of neurons in DRG.

**Keywords:** esketamine, nanoparticles, hyaluronic acid hydrogel, neuropathic pain

## Introduction

Neuropathic pain closely related to peripheral neuropathy or central sensitization is difficult to manage and treat.<sup>1,2</sup> Unbearable chronic pain not only brings great suffering to patients but also causes severe depression and even suicide.<sup>3</sup> However, the therapeutic effect of neuropathic pain is restricted, and few patients achieve sufficient remission.<sup>4</sup> General analgesic medications, including non-steroidal anti-inflammatory drugs (NSAIDs), cannot ameliorate neuropathic pain significantly and Opioids, represented by morphine, perform in a dose-dependent manner, and the call for de-opioidization is growing due to the common adverse effects such as tolerance and addiction.<sup>5,6</sup> Despite the recent research neuropathic pain has revealed numerous treatment targets, with few successful clinical applications, neuropathic pain remains challenging.<sup>7,8</sup>

Esketamine, the dextranomer of ketamine, is an N-methyl-D-aspartate (NMDA) receptor antagonist, and one of the few non-opioid potent analgesics in clinic.<sup>9</sup> Recent studies have shown that esketamine has a complex analgesic mechanism, acting on opioid receptors, monoamine receptors, M-cholinergic receptors, sodium channels, and calcium channels in addition to NMDA receptors.<sup>10-12</sup> It plays an important role in attenuating central sensitization associated with hyperalgesia, opioid tolerance, and chronic pain.<sup>13-15</sup> Although it has been reported that esketamine has a good effect on chronic pain, especially refractory neuropathic pain, its analgesic effect can

only last for several hours after administration due to its short half-life, inevitably requiring repeated administration or continuous infusion, which leads to poor patient compliance and inferior treatment.<sup>16–18</sup> In addition, there are certain side effects, such as delirium and hallucinations, associated with a single large dose of intravenous esketamine.<sup>19</sup> Therefore, it is significant to achieve sustained release of esketamine and prolong the analgesic effect.

In the present study, the Nanoparticle-Hydrogel Delivery System was developed to enhance the sustained release of esketamine, improve its efficacy and decrease the side effects. We explored the release efficiency of the delivery system *in vitro*, verified the drug distribution after release *in vivo*, and the mechanical allodynia induced by SNL was examined after spinal nerve root administration of the delivery system (Figure 1A–C). Specifically, we inject this system around the nerve root rather than intravenously or intrathecally. Further, we investigated the effect on neuronal excitability in DRG neurons and changes in astrocytes in the spinal cord after administration. In the end, we evaluated the biocompatibility and safety of the delivery system.

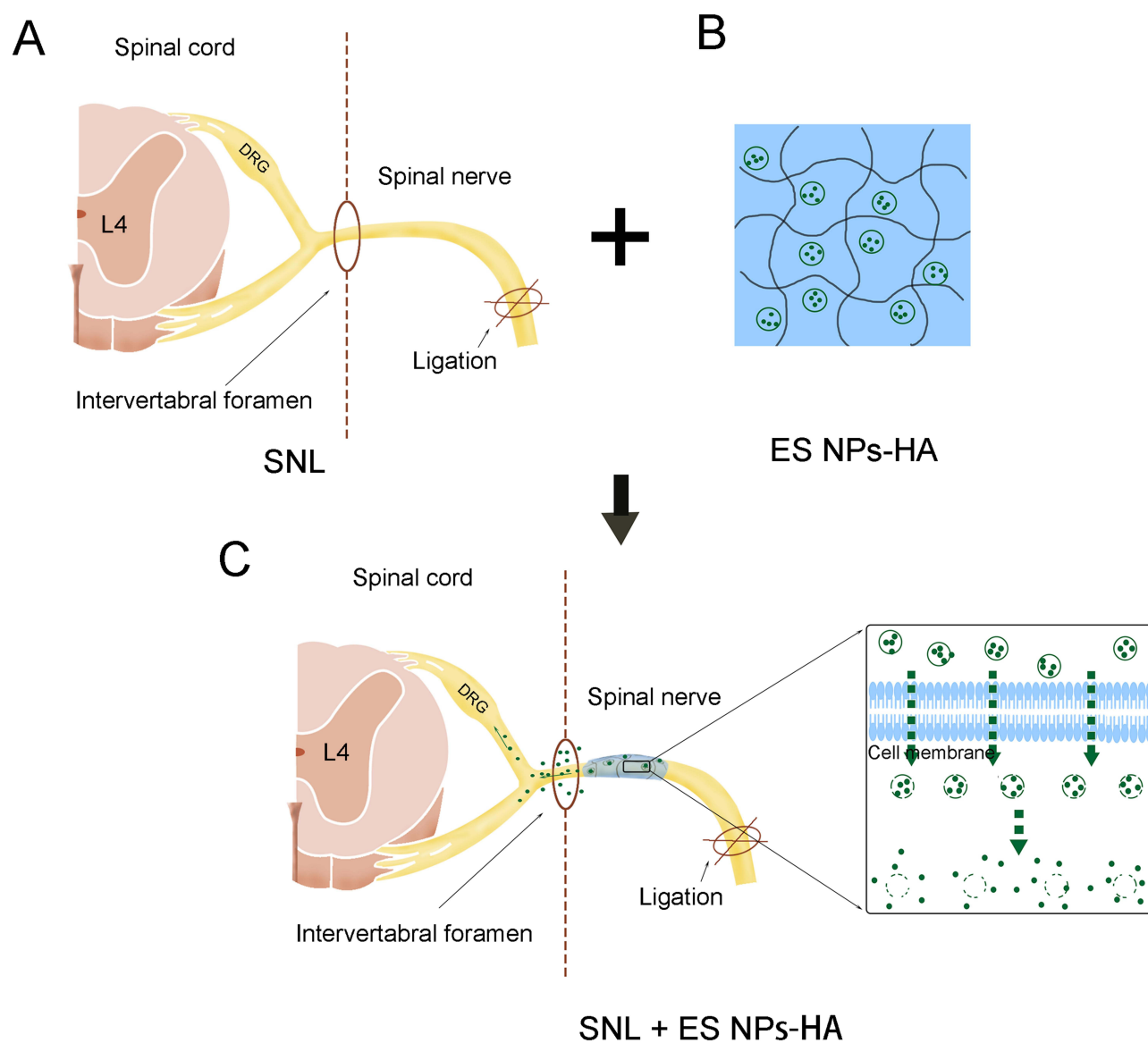


**Figure 1** Esketamine-encapsulated PLGA nanoparticles topical application diagram. Spinal nerve ligation in mice (A); ES NPs-HA: hydrogel-containing esketamine-encapsulated nanoparticles (B); Spinal nerve root administration (C).

## Materials and Methods

### Animals and Surgery

ICR mice (3–4 weeks) were bought from Nantong University's Animal Experimental Center (Jiangsu, China). Food and water are freely available. The animal facility is maintained at  $23^{\circ}\text{C} \pm 1^{\circ}\text{C}$  on a 12:12 h light-dark cycle. After the surgery, the mice were allowed to recover on a warming blanket. The Nantong University Experimental Animal Center's Animal Care Committee gave its approval to all experimental protocols (Approval No. S20210325-933). The animal experiments were performed in accordance with Regulations for the Administration of Affairs Concerning Experimental Animals (Order No. 2 of the State Science and Technology Commission of the People's Republic of China, 1988). The welfare of the laboratory animals followed in strict accordance with the guidelines for the Laboratory animal—Guideline for ethical review of animal welfare 《GB/T 35892–2018》.

Mice were anesthetized with pentobarbital sodium, and a paraspinal parallel incision was made after anesthesia to expose and remove the L6 transverse process to find the L4 and L5 spinal nerves, separate the L5 spinal nerves, ligate with 6–0 surgical silk, and expose only the L5 nerve without ligation in mice in the sham group. For spinal nerve root administration, after exposing the L5 spinal nerve, the L5 intervertebral foramen is sought, and the administration site is at the spinal nerve exiting the intervertebral foramen. The experiment was divided into four groups. Two groups of mice received esketamine (60 mg/kg) injection or 0.9% saline. The latter two groups received hydrogel-containing esketamine-encapsulated nanoparticles (50  $\mu\text{L}$ ) or hydrogel-containing 0.9% saline-encapsulated nanoparticles.

### Preparation of Esketamine-Encapsulated PLGA Nanoparticles

Nanoparticles containing esketamine were obtained by using the double emulsion solvent evaporation technique as described before,<sup>20</sup> with some modifications. In brief, 500  $\mu\text{L}$  of the esketamine solution (25 mg/mL, Jiangsu, China) was emulsified in 5 mL of dichloromethane containing 100 mg of PLGA (65:35 lactic acid to glycolic acid ratio, molecular weight = 40,000~75,000, Sigma-Aldrich) using a ultrasonic homogenator (Sonoplus HD 2070, Bandelin electronic, Berlin, Germany) for 1 min over an ice bath. Next, the mixture was injected into 18 mL of 1.5% PVA (poly(vinyl alcohol), molecular weight = 14,160) to form the double emulsion. The mixture was then re-emulsified for 1 min over an ice bath and then stirred for at least 24h at room temperature to evaporate the dichloromethane completely. The nanoparticles were collected and washed three times with distilled water by centrifugation at 15,000 rpm for 5 min. Lastly, the esketamine-encapsulated nanoparticles were then collected and resuspended in the phosphate-buffered saline.

### Synthesis of Thiol-Modified Hyaluronic Acid

Thiol-modified hyaluronic acid was synthesized by amidation reaction as described before.<sup>20</sup> Briefly, 384 mg of 1-(3-dimethylaminopropyl)-3-ethylcarbodiimide hydrochloride and 230 mg of N-hydroxysuccinimide were successively added to 80 mL of 1% hyaluronic acid sodium salt solution, then the pH was adjusted to 5.0. After stirring for 0.5h, 238 mg of 3'-30-dithiobis(propionohydrazide). The resulting solution was stirred at room temperature overnight. Thereafter, the pH of the reaction mixture was raised to 8.5. Then 772 mg of dithiothreitol was added to the above reaction solution. The reaction was carried out at room temperature for 12 h. The reaction mixture was adjusted with hydrochloric acid solution to 3.5. The mixture finally was dialyzed in membrane tubes (molecular weight cut-off of 12,000–14,000 Da) against acidified water (pH = 3.5) for 48 h. After dialysis, thiol-modified hyaluronic acid was obtained by freeze-drying.

### Synthesis of Polyethylene Glycol-Diacrylate

Polyethylene glycol-diacrylate was synthesized by an esterification reaction as described before.<sup>21</sup> Briefly, dry Polyethylene glycol (Mw 3000, 6 g, 4 mmol functional group) and triethylamine (606 mg, 6 mmol) were dissolved in 40 mL of dry dichloromethane. Acryloyl chloride (542 mg, 6 mmol) was added dropwise to the reaction solution under stirring. The reaction is conducted in dark conditions for 12 hours. The reaction product was filtered first, then precipitated with diethyl ether, and dried under vacuum conditions. The obtained product was further dissolved in

water and then extracted with dichloromethane. Finally, the obtained solution was precipitated by diethyl ether again, and the precipitate was dried under vacuum.

## Preparation of Hydrogel-Containing Esketamine-Encapsulated Nanoparticles

The esketamine-encapsulated nanoparticles embedded in hydrogel was prepared by cross-linking between thiol-modified hyaluronic acid and polyethylene glycol-diacrylate. Thiol-modified hyaluronic acid (320 mg, 0.8 mmol of disaccharide repeating units) was dissolved in 20 mL of phosphate-buffered saline containing esketamine-encapsulated nanoparticles. Then, 5 mL of polyethylene glycol-diacrylate (1.2 g, 0.4 mmol) aqueous solution was added in the above mixture and mixed for 0.5min. The formation of hydrogel-containing esketamine-encapsulated nanoparticles occurred within 0.5h.

## Characterization of Hydrogel-Containing Esketamine-Encapsulated Nanoparticles

The morphology of hydrogel-containing esketamine-encapsulated nanoparticles (ES NPs-HA) was observed by scanning electron microscopy (S-3400N; Hitachi, Tokyo, Japan). SEM: The esketamine-encapsulated nanoparticles were coated with platinum after freeze-drying, and then, they were observed under SEM. The average particle diameter and size distribution of esketamine-encapsulated nanoparticles was measured by DLS assay using a Brookhaven BI9000AT system (Brookhaven Instruments Corporation, Austin, TX, USA). DLS: The esketamine-encapsulated nanoparticles were first diluted in deionized water to a concentration of 0.1 mg/mL. The mean hydrodynamic diameter of esketamine-encapsulated nanoparticles was then determined by cumulative analysis.

## In vitro Drug Release from ES NPs-HA

First, 1 mL of esketamine solutions was prepared at concentrations of 0.5, 1.0, 1.5, 2.0, 2.5, 3.0, 3.5, and 4.0  $\mu\text{g/mL}$ . Absorbance values were detected at 269 nm using a multimode microplate reader (Molecular Devices) and absorbance concentration curves were plotted. 200  $\mu\text{L}$  of ES NPs-HA were collected and incubated in centrifuge tubes with 1 mL of PBS at 37°C. After collecting a portion of the mixed solution every 24 hours, replace it with a fresh PBS buffer. The absorbance values of the collected mixed solution were measured again using the multimode microplate reader and the daily dose of esketamine released was calculated from the absorbance-concentration curve previously plotted and repeated three times for 21 days. The cumulative release is summed over the daily releases for the corresponding number of days.

## Encapsulation Efficiency of the Esketamine-Encapsulated Nanoparticles

We measured the mass change of esketamine in the solution before and after drug encapsulation. After encapsulation, the amount of unencapsulated drug was present in the supernatant. The absorbance of the supernatant was measured at 269 nm using a multimode microplate reader and the amount of drug in the solution was calculated as the amount of unencapsulated drug. The equation for calculating the encapsulation rate of nanoparticles is as follows.

$$\text{Encapsulation efficiency (EE)(\%)} = \frac{\text{mass of drug} - \text{mass of unencapsulated drug}}{\text{mass of drug}} \times 100$$

## Pain Behavior Analysis

Prior to testing, all mice spent more than an hour each day for three consecutive days getting used to the same test environment. Mice were kept in a cage with a metal mesh floor for the duration of the test and given a half-hour window to acclimate. To stimulate the mice, increasing von Frey gradients were applied to the surgically ipsilateral hind paw's plantar surface (0.02–2.56 g), and Dixon's up-and-down method was used to calculate the animals' withdrawal threshold.<sup>21</sup> The behavioral tester was unaware of the grouping of mice.

## Whole-Cell Patch Clamp Recording of DRG Neurons

Briefly, surgically ipsilateral L4 DRG was rapidly removed from mice and placed in ice-cold Oxygenated artificial cerebrospinal fluid. Artificial cerebrospinal fluid formula (in mM):124 NaCl,1.25  $\text{NaH}_2\text{PO}_4$ , 26.0  $\text{NaHCO}_3$ ,1.0  $\text{MgCl}_2$ ,



2.0 CaCl<sub>2</sub>, 10.0 glucose, and 5 Hepes, pH 7.4. DRG surface fibers were removed microscopically and bisected, then transferred to a medium containing collagenase D (1.8 mg/mL; Roche) and trypsin (1 mg/mL; Ameresco) and incubated for 35 minutes at 37 °C in a thermostat. Then add 10% bovine fetal serum and blow the ganglion with a special 1 mL pipette tip. Dissociated neurons were seeded on poly-d-lysine coated dishes and supplemented with 10% fetal bovine serum and 30 ng/mL nerve growth factor and transferred to 95% and 5% carbon dioxide incubators at 37 °C for 6–8 hours.

The experiments were performed at room temperature. Small diameter neurons (<25nm) were selected for membrane clamp recording. The initial resistance of borosilicate glass patch pipettes is around 4–8MΩ. The pipette solution contained (in mM): 121 K-glucose, 20 KCl, 0.2 EGTA, 4.0 Na<sub>2</sub>ATP, 0.4 GTP-Tris, 2.0 MgCl<sub>2</sub>, and 10 Hepes, pH 7.3. The bath solution is same as artificial cerebrospinal fluid formula. Data were acquired using a Multiclamp 700B amplifier (Molecular Devices). pClamp software (version 10; Axon Instruments) was used for signal collection and analysis. Data was filtered at 2 kHz and digitized at 10 kHz using a data acquisition interface (1440A; Molecular Devices). The resting membrane potential and the action potential evoked by a series of ramp current stimulation (Time: 1 s; current intensity: 100, 200, and 300 pA) were recorded.

## Immunohistochemistry

Animals were anesthetized by deep inhalation and perfused with saline and 4% paraformaldehyde. The spinal cord was immediately removed from the lumbar region (L4-L6) and fixed overnight at 4°C. Sections were performed using a cryostat at 12 μm thickness (CM1950; Leica). Immunofluorescence staining was performed using the following primary antibody: GFAP (mouse, 1:500, Millipore, Burlington, MA), followed by incubation with alexa488-coupled secondary antibody (mouse, 1:1000, Jackson ImmunoResearch, West Grove, PA). Stained sections were examined using a Leica SP8 confocal microscope.

## Histology

Mice were executed 14 days after administration. Each incision site was exposed and L5 spinal nerve roots were collected, fixed in 10% paraformaldehyde, paraffin-embedded, sectioned, and stained with hematoxylin and eosin (H-E).

## Statistical Analysis

Results are expressed as mean ± SEM. All statistical results were analyzed with GraphPad Prism 6. Differences between multiple groups were determined by two-way repeated measures (RM) ANOVA. Bonferroni tests were used as post hoc tests when the ANOVA showed significant differences. Between-group analysis was completed using an unpaired Student's *t*-test. *p*-values <0.05 were considered statistically significant.

## Results

### Characterization of ES NPs-HA

Esketamine is rapidly metabolized in vivo, so we developed esketamine-encapsulated nanoparticles employing PLGA nanoparticles as carriers to provide continuous drug output.<sup>22</sup> SEM was used to examine the appearance and structural integrity of esketamine-encapsulated nanoparticles (Figure 2A). The size of their particles was 117.5 nm on average (Figure 2B). The EE of esketamine-encapsulated nanoparticles was 72.74 ± 4.11%. Then hydrogel-containing esketamine-encapsulated nanoparticles were prepared by cross-linking between thiol-modified hyaluronic acid and polyethylene glycol-diacrylate to increase drug release and decrease drug loss (Figure 2C). Finally, we obtained the ES NPs-HA, which provided the framework for steady and continuous drug release (Figure 2D).

### Release of ES NPs-HA in vitro

To detect the in vitro release efficiency of ES NPs-HA, we measured the absorbance of the complexes at 269 nm and plotted the absorbance-concentration standard curve (Figure 3A). Subsequently, the daily release rate of the nanocomposite at different pH values was measured at 37°C (Figure 3B). The release rate of ES NPs-HA was high in the first 3 days, and then

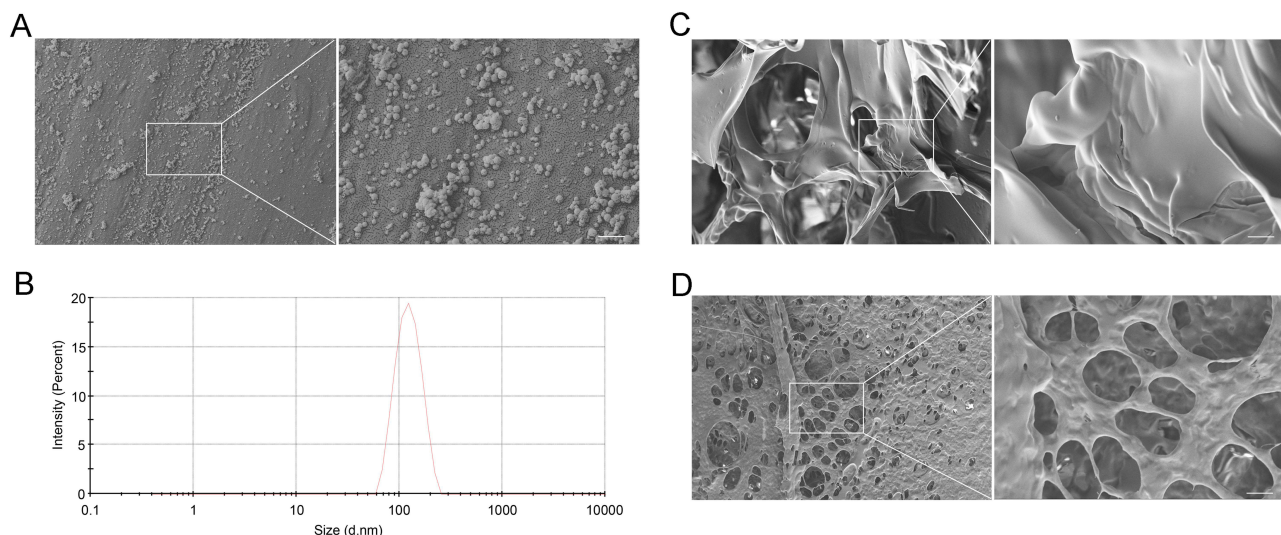


**Figure 2** The Characterization of ES NPs-HA. SEM images of the esketamine-encapsulated PLGA nanoparticles (A) Scale bar: 500 nm; Particle size distribution of esketamine-encapsulated PLGA nanoparticles (B); SEM images of hyaluronic acid hydrogel (C) Scale bar: 5  $\mu$ m; SEM images of ES NPs-HA (D) Scale bar: 5  $\mu$ m.

decreased stable and slowly. After 18 days, it was close to zero. The cumulative release rate diagram of the drug showed that the drug released more than 80% in 21 days, and most of the drugs were released in the first 14 days. The pH value (pH = 6.4) of the simulated inflammatory environment did not affect the release of the drug (Figure 3C).

### The Drug Distribution of ES NPs-HA in vivo

We further validated the uptake of ES NPs-HA in vivo. Since the PLGA esketamine-encapsulated nanoparticles are not fluorescent by themselves, we prepared rhodamine-conjugated PLGA nanoparticles with red fluorescence to follow their cellular uptake in real-time. Fluorescence detection on a postoperative day 5 showed that the ES NPs-HA could be absorbed by the encapsulated nerve roots (Figure 4A), a phenomenon not seen in the empty PLGA nanoparticles (Figure 4B). DAPI staining of the nuclei also did not reveal significant necrosis or effects on the structure and number of nuclei. This also indirectly indicates the safety of NPs-HA. Some loss may occur when nanoparticles are placed directly around the nerve. For more effective pain relief, we use the hydrogel- nanoparticles system that enriches the nanoparticles and reduces their dispersion, while the hydrogel provides a sustained release of the drug released from the nanoparticles.

### ES NPs-HA Attenuated SNL-Induced Pain Hypersensitivity

First, we established a spinal nerve ligation mouse model. As shown in Figure 5A, the drug was injected at the same time as the nerve roots were ligated, and the mice's pain behaviour was assessed for 21 days after the surgery. After 14 days,

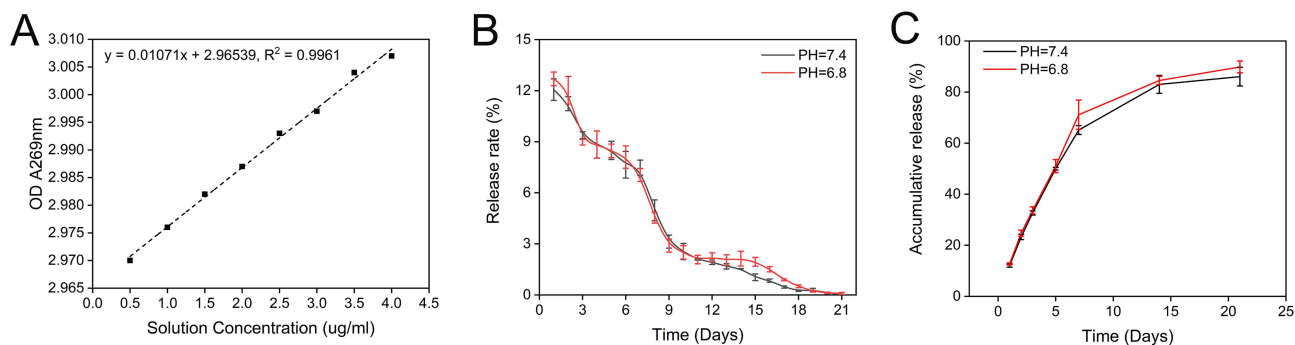


**Figure 3** In vitro drug release characteristics of ES NPs-HA. Standard Esketamine release curve. (A) Daily release of ES NPs-HA. (B) Cumulative release of ES NPs-HA (C).

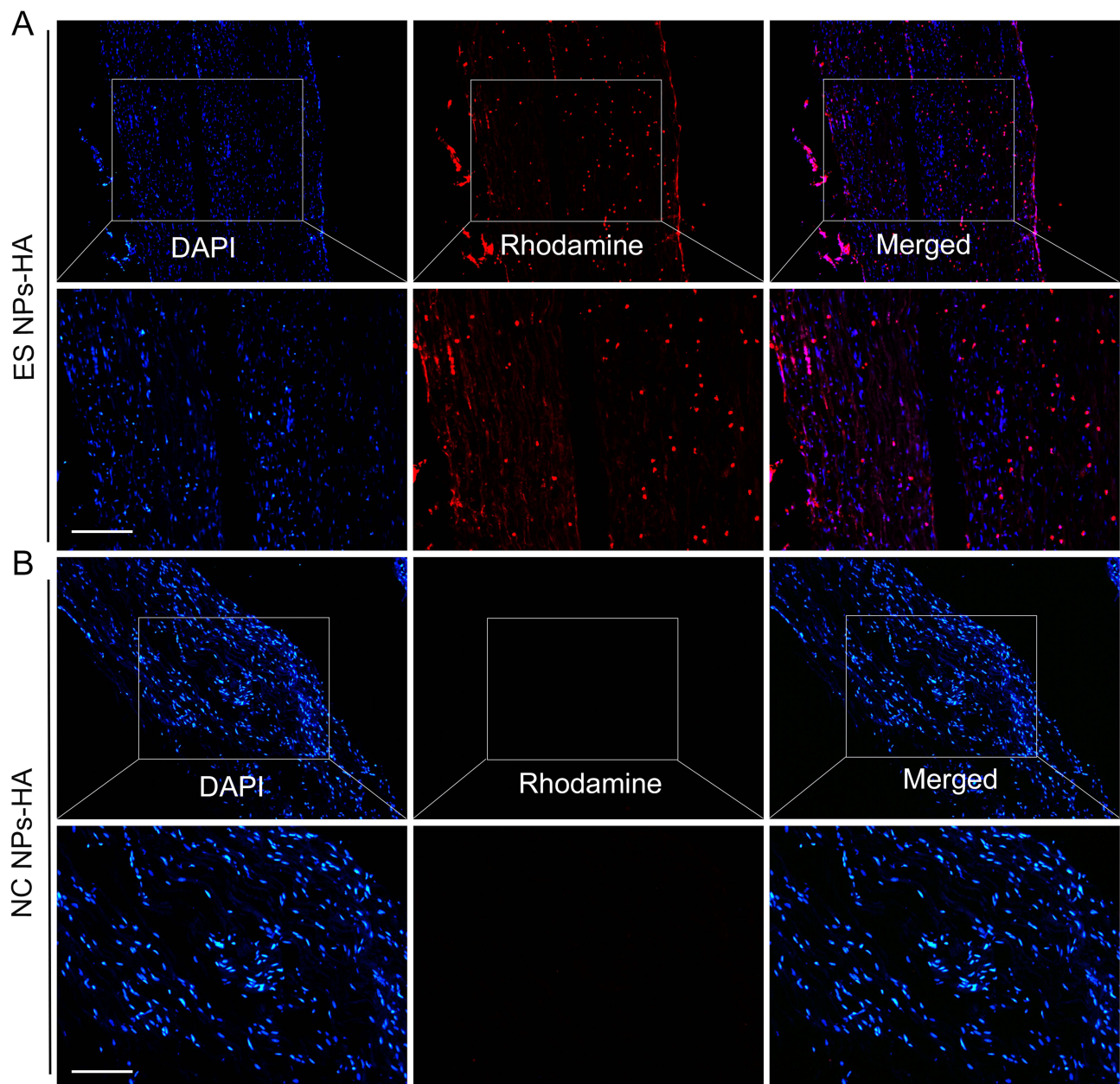


**Figure 4** In vivo uptake of nanoparticles. Rhodamine-conjugated PLGA nanoparticles were detected on postoperative day 5 (A); Empty PLGA nanoparticles (B). Scale bar: 50  $\mu$ m.

the nerve roots were sampled for histological examination. Compared with the preoperative period, mechanical pain thresholds were significantly lower in mice after ligation and persisted for more than 21 days (Figure 5B). Previous studies have shown that intrathecal or intraperitoneal injections of esketamine can attenuate SNL-induced pain behaviors.<sup>23,24</sup> However, this invasive intrathecal injection method has significant pitfalls for the spinal cord and cannot be used routinely in clinics.<sup>25</sup> The effect of the intraperitoneal injection is short-lived, and the dose is large. Wang et al showed that injection of PLGA-coated bupivacaine into the DRG reduced spinal nerve compression in mice for up to 14 days.<sup>26</sup> In the present study, we injected the drug into the spinal nerve roots. Nerve root blocks are common in the clinical treatment of neuropathic pain.<sup>27</sup> The nerve roots exiting from the intervertebral foramen are not only close to the DRG but might even affect the spinal cord. After spinal nerve ligation in mice, we injected esketamine at the nerve root and tested mechanical pain in mice 1–7 days after surgery. Mechanical pain thresholds were significantly higher in SNL+ES

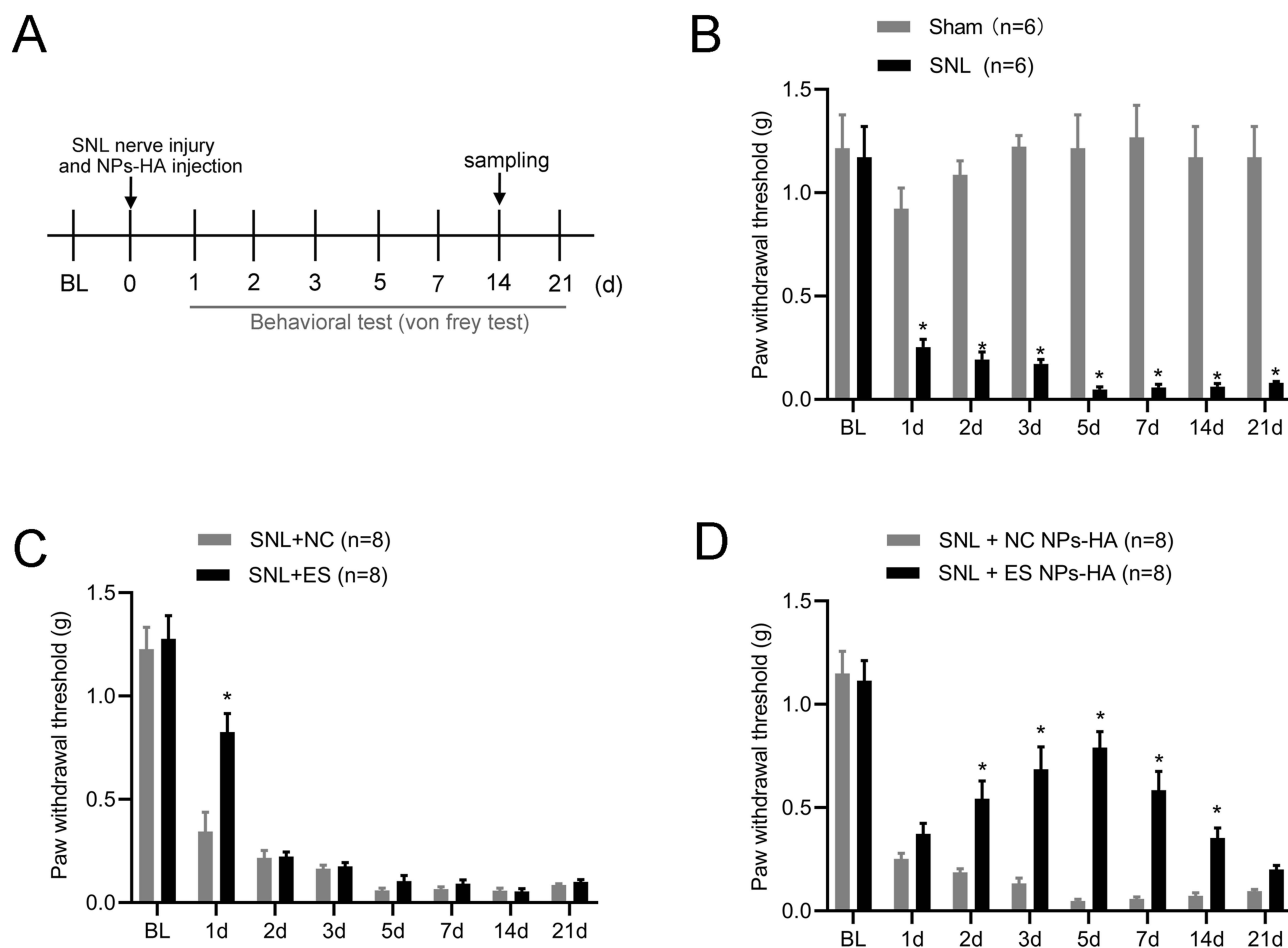


**Figure 5** Effect of ES NPs-HA on neuropathic pain. Experimental timeline of this study (A) Mechanical pain threshold in mice after spinal nerve ligation (B) (n=6/group); Effect of a single treatment of esketamine on mechanical pain in SNL mice (C) (n=8/group); The effect of ES NPs-HA administration on mechanical pain in SNL mice (D) (n=8/group). Data are expressed as the mean  $\pm$  SEM. \*P < 0.05; Two-way RM ANOVA followed by the Bonferroni test.

group compared to SNL+NC group, but this effect lasted for only one day (Figure 5C). To assess the analgesic effect of the ES NPs-HA, we placed it around the nerve roots outside the intervertebral foramen. Compared with SNL+NC NPs-HA group, the mechanical hypersensitivity of mice in SNL+ES NPs-HA group was relieved from day 2 and maintained for more than 14 days after spinal nerve ligation (Figure 5D). The above suggests that ES NPs-HA can attenuate SNL-induced nociceptive hypersensitivity.

## ES NPs-HA Reduced the Excitability of Neurons in the DRG of SNL Mice

A key factor in the emergence of neuropathic pain is the dorsal root ganglion.<sup>28</sup> The neurons in DRG are the primary sensory neurons of pain transmission.<sup>29</sup> Spinal nerve root administration of ES NPs-HA significantly enhanced the analgesic effect on SNL mice. It is possible that esketamine acts on the damaged peripheral nerves and affects the occurrence of spontaneous action potentials of DRG neurons and the development of mechanical ectopic pain. Of course, this requires further experiments to determine the diffusion of esketamine in vivo. In this study, we recorded the neurons of DRG in mice by patch clamp and compared evoked action potentials (APs) of neurons in DRG. The APs were substantially more responsive to 100, 200, and 300 pA ramp current stimulation following SNL compared to the Sham group. However, ES NPs-HA significantly reduced the increase in the number of APs caused by SNL nerve injury, at 200 pA and 300 pA ramp currents (Figure 6A). This suggests that ES NPs-HA can inhibit neuronal excitability by blocking axonal conduction directly or acting indirectly on the DRG. Figure 6B–E show the representative traces of action potentials in responding to 100, 200, and 300 pA



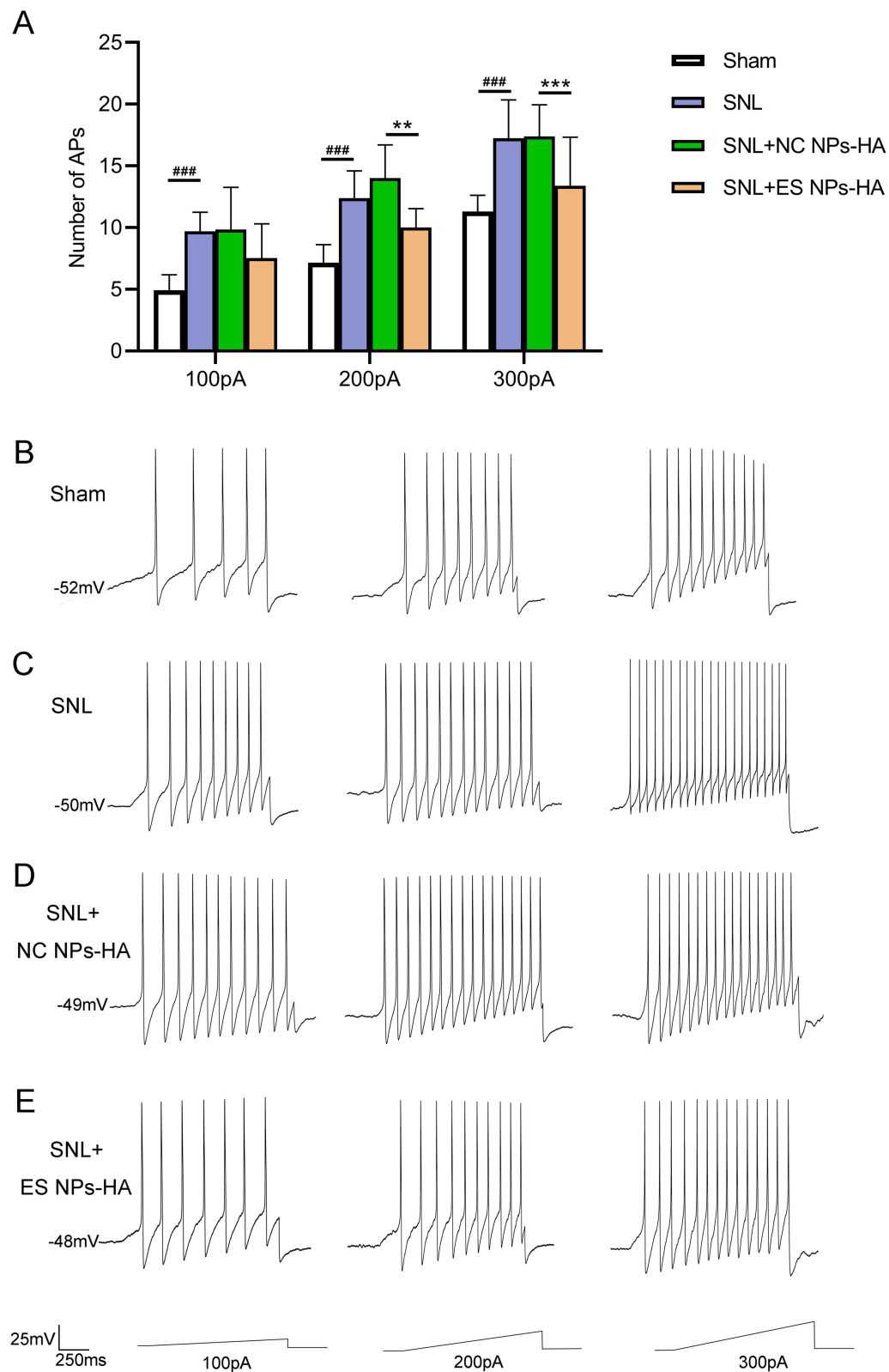


**Figure 6** Effect of ES NPs-HA on the excitability of DRG neurons in SNL mice. The number of Aps in DRG neurons of mice receiving ES NPs-HA treatment was recorded, 5 days after SNL (**A**); The representative traces of action potentials in responding to 100, 200, and 300 pA ramp current stimulation (**B–E**). Sham (**B**); SNL (**C**); SNL+NC NPs-HA (**D**); SNL+ES NPs-HA (**E**). \*\* $P < 0.01$ , \*\*\* $P < 0.001$ , vs SNL+NC Ps-HA; #### $P < 0.001$ , vs Sham. Two-way RM ANOVA followed by the Bonferroni test. Sham: Sham surgery group; SNL: Spinal nerve ligation group; SNL+NC NPs-HA: Injection of hydrogel-containing 0.9% saline-encapsulated nanoparticles after SNL; SNL+ES NPs-HA: Injection of hydrogel-containing esketamine-encapsulated nanoparticles after SNL.

ramp current stimulation. After ligation, the number of action potentials (APs) was significantly lower in the Sham group (Figure 6B) than in the SNL group (Figure 6C). This suggests that spinal nerve ligation affected the excitability of the neurons. There was also a significant decrease in the number of APs after injection of ES NPs-HA (Figure 6D). The saline encapsulated only did not have the same effect (Figure 6E). These are consistent with the statistical results in Figure 6A.

## ES NPs-HA Inhibited Excessive Activation of Mouse Spinal Astrocytes

Astrocytes are the most abundant glial cells in the nervous system, and when peripheral nerves are damaged, astrocytes are activated to participate in neuroinflammatory responses and pain sensitization.<sup>30,31</sup> Therefore, in this study, we examined the activation of astrocytes in the ipsilateral spinal dorsal horn after SNL. In SNL group, 5 days after spinal nerve ligation, immunofluorescence staining for astrocytes in the ipsilateral dorsal horn of the spinal cord increased significantly (Figure 7A and B). On the other hand, compared with SNL group, the immunofluorescence reaction of astrocytes in the ipsilateral spinal dorsal horn of SNL + ES NPs-HA group was significantly reduced (Figure 7C).

## The Safety of ES NPs-HA

At 14 days after surgery, the wound healing at the surgical site of the mice was normal. To evaluate the biological safety of the complexes, we performed HE staining on the nerve wrapped by ES NPs-HA. Compared with the control group (Figure 8A), there was no obvious inflammatory reaction in ES group (Figure 8B) and ES NPs-HA group (Figure 8C). The cells in the nerve root were evenly distributed, and there were no abnormal changes such as swelling or atrophy in the axons. This indicates that esketamine solution or ES NPs-HA has no significant effect on normal nerve tissue and the biocompatibility is well.

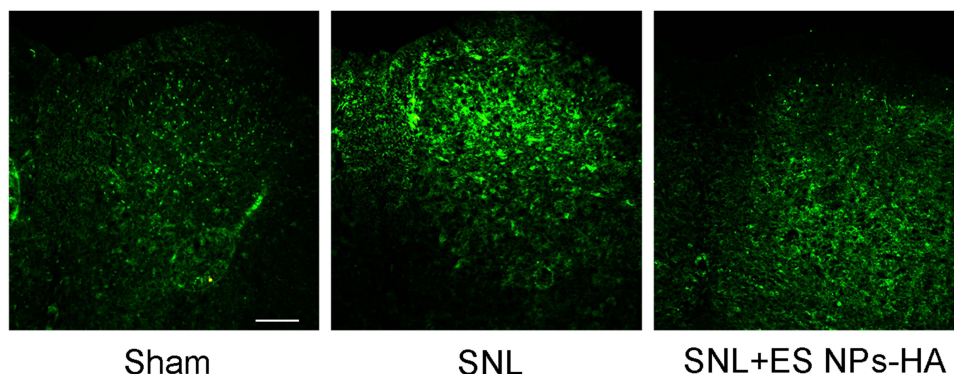


**Figure 7** Effect of ES NPs-HA on spinal astrocytes in mice. On day 5 postoperative, L4 spinal sections were taken and incubated with anti-GFAP antibodies. Sham (A); SNL (B); SNL+ES NPs-HA (C). Scale bar: 100  $\mu$ m.

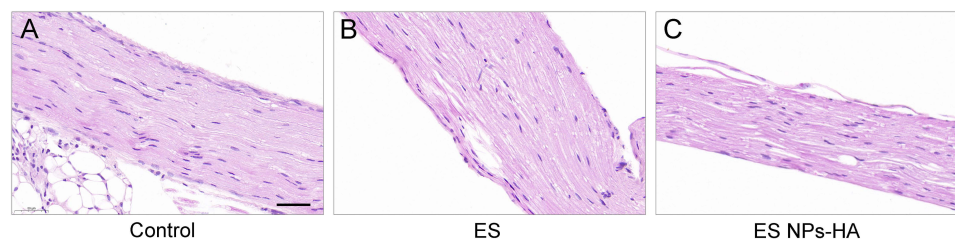


**Figure 8** Tissue reactions of ES NPs-HA. HE staining of nerves 14d after treatment with (A) Control: 0.9% NaCl, (B) ES: esketamine, or (C) ES NPs-HA: hydrogel-containing esketamine-encapsulated nanoparticles. Scale bar: 100  $\mu$ m.



## Discussion

As the exteroceptor of ketamine, the NMDA receptor is generally considered to be the main molecular target of esketamine.<sup>32</sup> This receptor is widely distributed in neuronal cells, closely influences neuronal development, and forms a prominent role in neuropathic pain and other CNS pathologies.<sup>33–35</sup> There are a lot of reports on the effects of ketamine on neurons, and Zeilhofer et al reported the effects of ketamine on NMDA receptor currents in cultured neurons.<sup>36</sup> In addition, ketamine can also inhibit neuronal excitability by blocking sodium and potassium channels inhibiting neuronal excitability.<sup>10,37</sup> In the present experiments, we recorded changes in the action potential of DRG neurons after administration, but further studies are needed on the targets of esketamine action on neurons. Further, more and more reports suggest that the effects of ketamine on the nervous system are not limited to neurons, but glial cells also play an important role. In cellular experiments *in vitro*, esketamine may alleviate pain by inhibiting calcium-activated potassium channels in microglia.<sup>38</sup> In a neuropathic pain model, a study reported that intrathecal ketamine injection inhibited SNL-induced astrocyte activation not inhibited by intraperitoneal ketamine.<sup>23</sup> In addition, it was shown that rapid morphological changes and serum BDNF levels in hippocampal astrocytes were associated with the injection of esketamine.<sup>39</sup> Ketamine has been repeatedly reported to inhibit astrocyte activation, in the central nervous system. Therefore, in the present experiments, we preliminarily verified the effect of ES NPs-HA on astrocytes in the spinal cord. The analgesic targets of esketamine are numerous and involve multiple signaling pathways. With continuous research, it has been one of the most promising drugs for the treatment of neuropathic pain.<sup>9,15,16</sup>

In the clinic, there are numerous sustained-release painkillers available, including tablets of diclofenac sodium, tramadol hydrochloride, and morphine hydrochloride. Lamotrigine loaded with PLGA as a drug carrier was utilized to demonstrate the analgesic impact of the drug in animal models, according to Lalani et al.<sup>40</sup> Additionally, it was shown by Kim, Shin et al that duloxetine nanoparticles might extend the analgesic effects of medications by improving microglial targeting.<sup>41</sup> Nanomaterials have emerged as a new direction in the development of pain medications.<sup>42</sup> Notably, Hyaluronic acid, used in a variety of biomedical research areas, is now a successful sustained-release method in drug delivery technology.<sup>43</sup> Nanoparticles in granular form, when applied topically, do not completely surround the nerve root and there is partial loss, which can be avoided to some extent with hydrogels. Hydrogels have some adhesive properties that allow nanoparticles to concentrate around the nerve, reducing drug loss and potentially showing better local effects. Also, Hydrogels can be drug release prolongers. Of course, more convincing evidence would require further research to prove this. To find a suitable encapsulation dose, we refer to the effective dose of intraperitoneal administration. Although the behavior of mice showed a good analgesic effect, this may not achieve the maximum benefit of the drug. The drug release curve was drawn by *in vitro* drug release detection and compared with PLGA, Nanoparticles-Hydrogel system showed a longer sustained release period. In addition to the slow-release properties, drugs encapsulated by nanoparticles have high delivery efficiency, especially in the blood-brain barrier of the central system.<sup>44,45</sup> A new approach to treating central disease-related neuropathic pain is provided by nanotechnology.<sup>46</sup>

Although intrathecal administration of esketamine relieved pain in SNL mice, it was potentially toxic to the brain and spinal cord.<sup>25</sup> Ketamine has been found to significantly increase synaptic apoptosis during brain development.<sup>47</sup> At the same time, we recognise that intrathecal drugs carry certain risks that are not taken into account in most animal testing, and it has been empirically observed that people with chronic cancer pain who take intrathecal ketamine exhibit severe histologic abnormalities.<sup>48</sup> These restrict the use of esketamine intraspinal. To treat neuropathic pain while minimizing unneeded side effects, medication sustained-release agents are inserted into the intervertebral foramen. This allows the medicine to travel to the invading nerve roots or ganglia and even to the nerve cells of the DRG. It might introduce fresh approaches to the existing management of intractable peripheral neuralgia, which could be useful in the treatment of conditions including postherpetic neuralgia, phantom limb pain, and postoperative pain.<sup>49,50</sup>

Only a few nanomedicines have received FDA approval, even though nanoparticles now hold considerable promise for pain management.<sup>51</sup> Its safety is frequently questioned. In this experiment, tissues in various regions of the body, including the spinal cord, should fall within the detection range in addition to detecting the local inflammatory reaction to the drug. More research is still needed to determine the safe encapsulation dose of nanomedicines, including an accurate assessment of drug concentrations in various organs. In addition, due to the particularity of the central nervous system,

the nanoparticles might be preferentially engulfed by microglia after the nanoparticles enter the central nervous system, which provides a new strategy for achieving targeted drug release and reducing the side effects of systemic application.<sup>52</sup>

In conclusion, we developed a novel esketamine/nanoparticle-hydrogel system. By injecting the system around the nerve root, it successfully reduced the pain caused by spinal nerve ligation in mice, and it is worth noting that the nano complex may produce an analgesic effect by affecting the excitability of neurons in the DRG and inhibiting the activation of astrocytes in the spinal cord. Our study is expected to provide some support for the clinical application of nanotechnology in neuropathic pain.

## Acknowledgment

This work was supported by the National Science Foundation of China (81701105), and the Postgraduate Research & Practice Innovation Program of Jiangsu Province, China (SJCX21- 1470).

## Disclosure

The authors report no conflicts of interest in this work.

## References

- Campbell JN, Meyer RA. Mechanisms of neuropathic pain. *Neuron*. 2006;52(1):77–92. doi:10.1016/j.neuron.2006.09.021
- Meacham K, Shepherd A, Mohapatra DP, Haroutounian S. Neuropathic pain: central vs. peripheral mechanisms. *Curr Pain Headache Rep*. 2017;21(6):28. doi:10.1007/s11916-017-0629-5
- IsHak WW, Wen RY, Naghdechi L, et al. Pain and depression: a systematic review. *Harv Rev Psychiatry*. 2018;26(6):352–363. doi:10.1097/HRP.0000000000000198
- Bannister K, Sachau J, Baron R, Dickenson AH. Neuropathic pain: mechanism-based therapeutics. *Annu Rev Pharmacol Toxicol*. 2020;60:257–274. doi:10.1146/annurev-pharmtox-010818-021524
- Rasmussen-Barr E, Held U, Grooten WJ, et al. Non-steroidal anti-inflammatory drugs for sciatica. *Cochrane Database Syst Rev*. 2016;10(10):CD012382. doi:10.1002/14651858.CD012382
- Garland EL. Treating chronic pain: the need for non-opioid options. *Expert Rev Clin Pharmacol*. 2014;7(5):545–550. doi:10.1586/17512433.2014.928587
- Gangadhar M, Mishra RK, Sriram D, Yogeewari P. Future directions in the treatment of neuropathic pain: a review on various therapeutic targets. *CNS Neurol Disord Drug Targets*. 2014;13(1):63–81. doi:10.2174/18715273113126660192
- Attal N, Bouhassira D. Translational neuropathic pain research. *Pain*. 2019;160(Suppl 1):S23–S28. doi:10.1097/j.pain.0000000000001522
- Yang Y, Maher DP, Cohen SP. Emerging concepts on the use of ketamine for chronic pain. *Expert Rev Clin Pharmacol*. 2020;13(2):135–146. doi:10.1080/17512433.2020.1717947
- Robinson B, Gu Q, Kanungo J. Antidepressant actions of ketamine: potential role of l-type calcium channels. *Chem Res Toxicol*. 2021;34(5):1198–1207. doi:10.1021/acs.chemrestox.0c00411
- Wagner LE, Gingrich KJ, Kulli JC, Yang J. Ketamine blockade of voltage-gated sodium channels: evidence for a shared receptor site with local anesthetics. *Anesthesiology*. 2001;95(6):1406–1413. doi:10.1097/0000542-200112000-00020
- Lavender E, Hirasawa-Fujita M, Domino EF. Ketamine's dose related multiple mechanisms of actions: dissociative anesthetic to rapid antidepressant. *Behav Brain Res*. 2020;390:112631. doi:10.1016/j.bbr.2020.112631
- Porter SB, Schwenk ES. Ketamine and remote hyperalgesia. *Minerva Anesthesiol*. 2018;84(4):432–433. doi:10.23736/S0375-9393.18.12521-1
- Luginbühl M, Gerber A, Schnider TW, Petersen-Felix S, Arendt-Nielsen L, Curatolo M. Modulation of remifentanyl-induced analgesia, hyperalgesia, and tolerance by small-dose ketamine in humans. *Anesth Analg*. 2003;96(3):726–732. doi:10.1213/01.ANE.0000048086.58161.18
- Niesters M, Martini C, Dahan A. Ketamine for chronic pain: risks and benefits. *Br J Clin Pharmacol*. 2014;77(2):357–367. doi:10.1111/bcp.12094
- Culp C, Kim HK, Abdi S. Ketamine use for cancer and chronic pain management. *Front Pharmacol*. 2021;11:599721. doi:10.3389/fphar.2020.599721
- Kamp J, van Velzen M, Aarts L, Niesters M, Dahan A, Olofsen E. Stereoselective ketamine effect on cardiac output: a population pharmacokinetic/pharmacodynamic modelling study in healthy volunteers. *Br J Anaesth*. 2021;127(1):23–31. doi:10.1016/j.bja.2021.02.034
- Pickering G, Morel V, Micallef J. Kétamine et douleur chronique: une revue narrative de son efficacité et sécurité [Ketamine and chronic pain: a narrative review of its efficacy and its adverse events]. *Thérapie*. 2018;73(6):529–539. doi:10.1016/j.therap.2018.06.001
- Cvrcek P. Side effects of ketamine in the long-term treatment of neuropathic pain. *Pain Med*. 2008;9(2):253–257. doi:10.1111/j.1526-4637.2007.00314.x
- Zhou YL, Yang QQ, Yan YY, Zhu C, Zhang L, Tang JB. Localized delivery of miRNAs targets cyclooxygenases and reduces flexor tendon adhesions. *Acta Biomater*. 2018;70:237–248. doi:10.1016/j.actbio.2018.01.047
- Dixon WJ. Efficient analysis of experimental observations. *Annu Rev Pharmacol Toxicol*. 1980;20:441–462. doi:10.1146/annurev.pa.20.040180.002301
- Wang J, Huang J, Yang S, et al. Pharmacokinetics and safety of esketamine in Chinese patients undergoing painless gastroscopy in comparison with ketamine: a randomized, open-label clinical study. *Drug Des Devel Ther*. 2019;13:4135–4144. doi:10.2147/DDDT.S224553
- Mei XP, Zhang H, Wang W, et al. Inhibition of spinal astrocytic c-Jun N-terminal kinase (JNK) activation correlates with the analgesic effects of ketamine in neuropathic pain. *J Neuroinflammation*. 2011;8(1):6. doi:10.1186/1742-2094-8-6
- Mei X, Wang W, Wang W, et al. Inhibiting astrocytic activation: a novel analgesic mechanism of ketamine at the spinal level? *J Neurochem*. 2009;109(6):1691–1700. doi:10.1111/j.1471-4159.2009.06087.x

25. Vranken JH, Troost D, de Haan P, et al. Severe toxic damage to the rabbit spinal cord after intrathecal administration of preservative-free S (+)-ketamine. *Anesthesiology*. 2006;105(4):813–818. doi:10.1097/0000542-200610000-00028
26. Wang T, Hurwitz O, Shimada SG, et al. Anti-nociceptive effects of bupivacaine-encapsulated PLGA nanoparticles applied to the compressed dorsal root ganglion in mice. *Neurosci Lett*. 2018;668:154–158. doi:10.1016/j.neulet.2018.01.031
27. Hayek SM, Shah A. Nerve blocks for chronic pain. *Neurosurg Clin N Am*. 2014;25(4):809–817. doi:10.1016/j.nec.2014.07.006
28. Esposito MF, Malayil R, Hanes M, Deer T. Unique characteristics of the dorsal root ganglion as a target for neuromodulation. *Pain Med*. 2019;20(Suppl 1):S23–S30. doi:10.1093/pm/pnz012
29. Berta T, Qadri Y, Tan PH, Ji RR. Targeting dorsal root ganglia and primary sensory neurons for the treatment of chronic pain. *Expert Opin Ther Targets*. 2017;21(7):695–703. doi:10.1080/14728222.2017.1328057
30. Colombo E, Farina C. Astrocytes: key regulators of neuroinflammation. *Trends Immunol*. 2016;37(9):608–620. doi:10.1016/j.it.2016.06.006
31. Chen YL, Feng XL, Cheung CW, Liu JA. Mode of action of astrocytes in pain: from the spinal cord to the brain. *Prog Neurobiol*. 2022;219:102365. doi:10.1016/j.pneurobio.2022.102365
32. Sinner B, Graf BM. Ketamine. *Handb Exp Pharmacol*. 2008;(182):313–333. doi:10.1007/978-3-540-74806-9\_15
33. Michaelis EK. Two different families of NMDA receptors in mammalian brain: physiological function and role in neuronal development and degeneration. *Adv Exp Med Biol*. 1993;341:119–128. doi:10.1007/978-1-4615-2484-7\_11
34. Deng M, Chen SR, Pan HL. Presynaptic NMDA receptors control nociceptive transmission at the spinal cord level in neuropathic pain. *Cell Mol Life Sci*. 2019;76(10):1889–1899. doi:10.1007/s00018-019-03047-y
35. McDonald JW, Silverstein FS, Johnston MV. Neurotoxicity of N-methyl-D-aspartate is markedly enhanced in developing rat central nervous system. *Brain Res*. 1988;459(1):200–203. doi:10.1016/0006-8993(88)90306-x
36. Zeilhofer HU, Swandulla D, Geisslinger G, Brune K. Differential effects of ketamine enantiomers on NMDA receptor currents in cultured neurons. *Eur J Pharmacol*. 1992;213(1):155–158. doi:10.1016/0014-2999(92)90248-3
37. Haeseler G, Tezlaff D, Buffer J, et al. Blockade of voltage-operated neuronal and skeletal muscle sodium channels by S (+)- and R(-)-ketamine. *Anesth Analg*. 2003;96(4):1019–1026. doi:10.1213/01.ANE.0000052513.91900.D5
38. Hayashi Y, Kawaji K, Sun L, et al. Microglial Ca (2+)-activated K (+) channels are possible molecular targets for the analgesic effects of S-ketamine on neuropathic pain. *J Neurosci*. 2011;31(48):17370–17382. doi:10.1523/JNEUROSCI.4152-11.2011
39. Ardalan M, Elfving B, Rafati AH, et al. Rapid effects of S-ketamine on the morphology of hippocampal astrocytes and BDNF serum levels in a sex-dependent manner. *Eur Neuropsychopharmacol*. 2020;32:94–103. doi:10.1016/j.euroneuro.2020.01.001
40. Lalani J, Patil S, Kolate A, Lalani R, Misra A. Protein-functionalized PLGA nanoparticles of lamotrigine for neuropathic pain management. *AAPS PharmSciTech*. 2015;16(2):413–427. doi:10.1208/s12249-014-0235-3
41. Kim SI, Shin J, Tran Q, et al. Application of PLGA nanoparticles to enhance the action of duloxetine on microglia in neuropathic pain. *Biomater Sci*. 2021;9(18):6295–6307. doi:10.1039/d1bm00486g
42. Babaie S, Taghivimi A, Hong JH, Hamishehkar H, An S, Kim KH. Recent advances in pain management based on nanoparticle technologies. *J Nanobiotechnology*. 2022;20(1):290. doi:10.1186/s12951-022-01473-y
43. Vasvani S, Kulkarni P, Rawtani D. Hyaluronic acid: a review on its biology, aspects of drug delivery, route of administrations and a special emphasis on its approved marketed products and recent clinical studies. *Int J Biol Macromol*. 2020;151:1012–1029. doi:10.1016/j.ijbiomac.2019.11.066
44. Zhou Y, Peng Z, Seven ES, Leblanc RM. Crossing the blood-brain barrier with nanoparticles. *J Control Release*. 2018;270:290–303. doi:10.1016/j.jconrel.2017.12.015
45. Feng J, Lepetre-Mouelhi S, Gautier A, et al. A new painkiller nanomedicine to bypass the blood-brain barrier and the use of morphine. *Sci Adv*. 2019;5(2):eaau5148. doi:10.1126/sciadv.aau5148
46. da Silva A, Lepetre-Mouelhi S, Couvreur P. Micro- and nanocarriers for pain alleviation. *Adv Drug Deliv Rev*. 2022;187:114359. doi:10.1016/j.addr.2022.114359
47. Hashimoto K. Detrimental side effects of repeated ketamine infusions in the brain. *Am J Psychiatry*. 2016;173(10):1044–1045. doi:10.1176/appi.ajp.2016.16040411
48. Vranken JH, Troost D, Wegener JT, Kruijs MR, van der Vegt MH. Neuropathological findings after continuous intrathecal administration of S (+)-ketamine for the management of neuropathic cancer pain. *Pain*. 2005;117(1–2):231–235. doi:10.1016/j.pain.2005.06.014
49. Lin CS, Lin YC, Lao HC, Chen CC. Interventional treatments for postherpetic neuralgia: a systematic review. *Pain Physician*. 2019;22(3):209–228. doi:10.36076/ppj/2019.22.209
50. Collins KL, Russell HG, Schumacher PJ, et al. A review of current theories and treatments for phantom limb pain. *J Clin Invest*. 2018;128(6):2168–2176. doi:10.1172/JCI94003
51. Bobo D, Robinson KJ, Islam J, Thurecht KJ, Corrie SR. Nanoparticle-based medicines: a review of FDA-approved materials and clinical trials to date. *Pharm Res*. 2016;33(10):2373–2387. doi:10.1007/s11095-016-1958-5
52. Zhao N, Francis NL, Calvelli HR, Moghe PV. Microglia-targeting nanotherapeutics for neurodegenerative diseases. *APL Bioeng*. 2020;4(3):30902. doi:10.1063/5.0013178